**TABLE 3 Specifications of the Proposed 14-Pole Filter**

| Specification | Measured | Simulated |
|---|---|---|
| Center frequency $f_0$ | 830 MHz | 830 MHz |
| Passband bandwith | 11.2 MHz | 12 MHz |
| Return loss | −24 dB | −23 dB |
| Insertion loss | ≤0.5 dB | ≤0.1 dB |
| Transmit band rejection | ≥70 dB | ≥70 dB |
| GD variation < ± 5 ns | $f_0$ ± 3.5 MHz | $f_0$ ± 3.3 MHz |
| GD variation < ± 10 ns | $f_0$ ± 3.95 MHz | $f_0$ ± 3.9 MHz |
| GD variation < ± 20 ns | $f_0$ ± 4.55 MHz | $f_0$ ± 4.5 MHz |

tends to be sensitive to the tolerances in both the design and fabrication, some related sensitivity analyses based on the proposed parameters have been performed, and it is found that the tuning distortion caused by the variation of resonant frequency of each resonator have some noticeable effect on the desired response.

## 4. CONCLUSION

This letter presents the synthesis of a narrow-band bandpass filter for CDMA2000 communications systems, which has a 14-pole general Chebyshev function response with a passband of 11.2 MHz at 830 MHz. The coupling matrix of the filter is derived from cost function using nonlinear LM algorithm. The filter response with two pairs of TZs for group delay self-equalization and one pair of TZs at finite frequencies for high selectivity requirement is implemented by using three CQ coupling structures. The frequency responses demonstrating a good agreement between the measured and the simulated specifications are obtained. The proposed method can be further exploited for various mobile communication system applications.

## ACKNOWLEDGMENTS

This work was supported by the National High Technology Research and Development Program of China (Grant No. 2006AA03Z235). The authors also thank for the Postdoctoral Research Funds of Tianjin 2009, China.

## REFERENCES


1. A.E. Atia and A.E. Williams, New type of waveguide band pass filters for satellite transponders, COMSAT Tech Rev 1 (1971), 21–43.
2. R.J. Cameron, Advanced coupling matrix synthesis techniques for microwave filters, IEEE Trans Microwave Theory Tech 51 (2003), 1–10.
3. S. Amari, Synthesis of cross-coupled resonator filters using an analytical gradient-based optimization technique, IEEE Trans Microwave Theory Tech 48 (2000), 1559–1564.
4. C-K. Liao and C-Y. Chang, Design of microstrip quadruplet filters with source-load coupling, IEEE Trans Microwave Theory Tech 53 (2005), 2302–2308.
5. V. Miraftab and R.R. Mansour, Computer-aided tuning of microwave filters using fuzzy logic, IEEE Trans Microwave Theory Tech 50 (2002), 2781–2788.
6. V. Miraftab and M. Yu, Generalized lossy microwave filter coupling matrix synthesis and design using mixed technologies, IEEE Trans Microwave Theory Tech 56 (2008), 3016–3027.
7. G. Macchiarella, Accurate synthesis of inline prototype filters using cascaded triplet and quadruplet sections, IEEE Trans Microwave Theory Tech 50 (2002), 1779–1783.
8. J-S. Hong and M.J. Lancaster, Microstrip filters for RF/microwave applications, Wiley, New York, 2001.




# INTERFEROMETRY TECHNIQUE FOR REFRACTIVE INDEX MEASUREMENTS AT SUBCENTIMETER WAVELENGTHS

**N. A. Andrushchak,[1] O. I. Syrotynsky,[1] I. D. Karbovnyk,[2] Ya. V. Bobitskii,[1] A. S. Andrushchak,[1] and A. V. Kityk[3]**
[1] Lviv Polytechnic National University, 12 S. Bandery str., Lviv 79013, Ukraine
[2] Department of Electronics, Ivan Franko National University of Lviv, 107 Tarnavskogo str., Lviv 79017, Ukraine
[3] Faculty of Electrical Engineering, Czestochowa University of Technology, Al. Armii Krajowej 17, PL 42200, Czestochowa, Poland; Corresponding author: kityk@ap.univie.ac.at

*Received 29 July 2010*

**ABSTRACT:** *We demonstrate the interferometry technique for the refractive index measurements at subcentimeter wavelengths. The method is based on a path length sweeping being introduced into one of the interferometer arms, while the sample is tilted out of its normal position with respect to the incident electromagnetic radiation. The determination of the refractive index is realized through the recording of the interference patterns at several tilt angles.* © 2011 Wiley Periodicals, Inc. Microwave Opt Technol Lett 53:1193–1196, 2011; View this article online at wileyonlinelibrary.com. DOI 10.1002/mop.25944

**Key words:** *refractive index; subcentimeter wavelengths; interferometry technique*

## 1. INTRODUCTION

Electromagnetic radiation at centimeter and millimeter wavelengths [ultra-high frequency (UHF) 1–300 GHz] is widely used in many areas of the microwave and radiofrequency techniques. Most often, it is exploited in the radar and telecommunication applications. Since the last decade, the telecommunication technology develops intensively in the direction of higher frequencies having a goal of improving the data transfer speed. This stimulates a search for new functional materials suitable for the production of highly efficient antennas and radars in the UHF region. The dielectric constant $\varepsilon$ (or the refractive index $n = \varepsilon^{1/2}$) in that frequency range represent, in fact, one of the most important characteristics for such materials playing a key role in telecommunication technology. Precise determination of $\varepsilon$ and $n$ is strongly required by both designers and manufacturers of antenna and radar systems, therefore, numerous efforts that have been put in development of different laboratory setups. An advantage has been given to various resonator techniques, such as the open resonator systems (ORS) [1, 2] or the dispersive Fourier transform spectrometers (DFTS) [3–5], rather than to the waveguide (WG) methods [6–8]. In particular, the WG technique requires a specific preparation of the sample under test, whereas the air gap between the WG and the sample usually leads to a large error in the measurement result. In comparison, the resonator technique may be considered as one of the most accurate methods being applied at the millimeter–submillimeter wavelengths to study transparent materials. The great advantage of DFTS is that this is the only known technique, which simultaneously measures both the refractive index and the absorption coefficient with a high precision [3, 5]. There are also several other methods described (e.g., in Refs. 9–11), but their accuracy is considerably lower comparing to DFTS or even ORS techniques.

In this work, we demonstrate the interferometry technique suitable for the precise refractive index measurements at subcentimeter wavelengths. Unlike the resonant methods described

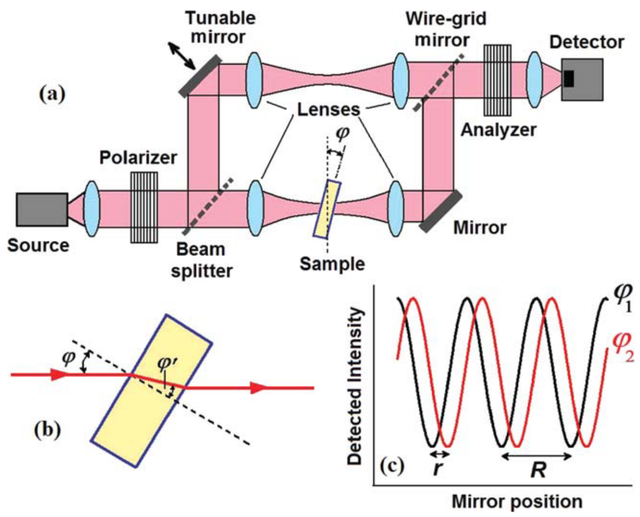


**Figure 1** Laboratory setup for the refractive index measurements in subcentimeter range of the electromagnetic radiation based on the Mach–Zehnder interferometer (a); the refraction of the electromagnetic wave at the sample edges ($\sin\varphi/\sin\varphi' = n$) (b); and schematic representation of the interference pattern shift due to a rotation of the sample from its initial angular position ($\varphi = \varphi_1$) to the final one ($\varphi = \varphi_2$) (c). [Color figure can be viewed in the online issue, which is available at wileyonlinelibrary.com]

above, which record the interference pattern by a wavelength sweeping, the registration of the interference fringes in our method is performed at the fixed wavelength of the coherent UHF radiation. It is based on a path-length sweeping being introduced into one of the interferometer arms while the sample is tilted out of its normal position with respect to the incident electromagnetic radiation. The refractive index is determined by the recording of the interference pattern at several tilt angles.

## 2. LABORATORY SETUP

Figure 1 shows the laboratory setup. It is based on the Mach–Zehnder interferometer and is quite similar to the one described in Ref. 12. The UHF radiation ($f = 33$ GHz) is generated by the Gunn's diode and consequently is collimated by means of the plastic lenses being set in both arms of the interferometer. The parallel-plate sample is placed into one arm of the interferometer and attached to the goniometric table providing the possibility of its angular orientation with the precision of about 0.01°. To change the effective path length in one of the interferometer arms, the tunable mirror can be displaced by means of the stepper motor, operated via the personal computer. If the measured samples are anisotropic, the grating polarizer and analyzer should be added into the setup as shown in Figure 1. By sweeping the position of the tunable mirror, one obtains the interferometric fringes being registered by the detector. Accordingly, the refractive index can be determined by measuring the distance between the neighbor fringes, $R$, and the shift of the interference pattern, $r$, which occurs due to a sample rotation from the initial angular position, $\varphi_1$, to the final position, $\varphi_2$. In the following, we derive the equation required for the determination of the refractive index by the interference turning method. Such equation appears to be considerably simplified if one of the angular positions, lets say $\varphi_1$, is set to zero, that is, one deals in this case with the UHF wave incident normally to the sample faces. Hereafter, we will address it as zero position (ZP). The sample set to ZP ($\varphi_1 = 0$) induces the optical path length:

$$\Delta(0) = nd, \tag{1}$$

where $d$ is the sample thickness. On the other hand, the sample being tilted by the angle $\varphi_2 = \varphi$ (see Fig. 1) is characterized by the induced path length $\Delta(\varphi)$, which reads as:

$$\Delta(\varphi) = nd/\cos\varphi' + d - d\cos(\varphi - \varphi')/\cos\varphi', \tag{2}$$

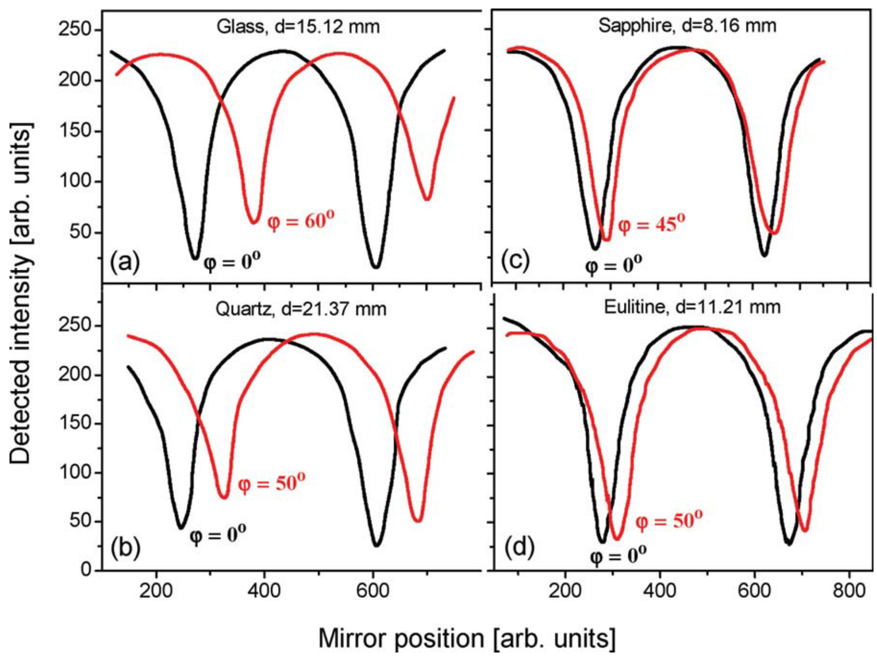


**Figure 2** Interferograms of several samples made of different materials being measured by means of the laboratory setup shown in Figure 1. The black curves are the interferograms recorded for the samples being set in ZP. The red curves are the interferograms measured for the samples tilted out from ZP by an angle $\varphi$. The magnitude of the tilt angle $\varphi$ and sample thickness $d$ are specified in each panel. (a) Glass, (b) quartz ($SiO_2$), (c) sapphire ($Al_2O_3$), and (d) eulitine ($Bi_4Ce_3O_{12}$). [Color figure can be viewed in the online issue, which is available at wileyonlinelibrary.com]

TABLE 1 The Magnitudes of the Refractive Index $n$ as Determined from the Interferograms Shown in Figure 2 ($f$ = 33 GHz) and Measured in Refs. 15–19 at $f$ = 300 GHz

| Frequency (GHz) | Optical Glass | Quartz ($SiO_2$) | Sapphire ($Al_2O_3$) | Eulitine ($Bi_4Ge_3O_{12}$) | Notes |
|---|---|---|---|---|---|
| 33 | 1.53 | 2.12 | 3.11 | 2.02 | Present work |
| 300 | 1.6 | 2.15 | 3.15 | – | Reported by Volkov, Prokhorov et al. [15–19] |

where $\varphi'$ is the refraction angle defined by Snell's law. For the details regarding the derivation of Eq. (2), we refer readers to the recent publications [13, 14]. The difference in the optical path lengths $\delta\Delta = \Delta(\varphi) - \Delta(0)$ may be determined from the interference pattern shift, whereas the sample is turned out from its ZP on the angle $\varphi$. Accordingly, it can be expressed as:

$$\delta\Delta = r\lambda/R, \tag{3}$$

where $\lambda$ is the wavelength of the UHF radiation. Considering Eqs. (1)–(3) together one obtains the refractive index of the sample:

$$n = \frac{\sin^2\varphi + Z^2}{2Z}, \tag{4}$$

where $Z$ value is:

$$Z = 1 - \cos\varphi - \frac{r\lambda}{Rd}. \tag{5}$$

## 3. TEST AND MEASUREMENTS

The laboratory setup shown in Figure 1 has been tested for several selected materials, both amorphous and crystalline ones. The measured interferograms of the glass, crystal quartz ($SiO_2$), sapphire ($Al_2O_3$), and eulitine ($Bi_4Ce_3O_{12}$) are shown in Figures 2(a), 2(b), 2(c), and 2(d), respectively. The black curves are the interferograms measured for the samples being set in ZP, whereas the red ones are the interferograms obtained for the samples tilted out from ZP by an angle $\varphi$. The tilt angle $\varphi$ and the sample thickness $d$ are specified for each measured sample in a corresponding panel of Figure 2. Determining the distance between the neighbor fringes $R$ and the shift of the interference pattern $r$, which occurs due to the sample tilting from its ZP, one obtains the refractive index $n$ by means of the Eqs. (4) and (5). Table 1 lists the magnitudes of the refractive indices $n$ measured in this work at $f$ = 33 GHz, and similarly, the refractive indices of the same materials as determined by Volkov et al. and Prokhorov et al. [15–18] at $f$ = 300 GHz. One can see that the dielectric properties of these materials at submillimeter–subcentimeter wavelengths exhibit a weak frequency dispersion resulting in a rather small decreasing of the refractive index as frequency lowers from 300 to 33 GHz. The accuracy of the refractive index determination is, in our case, defined mainly by the errors of measured tilt angle $\delta\varphi$, interferogram characteristics $\delta R$ and $\delta r$, sample thickness $\delta\delta$, and by the wavelength instability of the UHF source $\delta\lambda$. According to [19], the integral error $\delta n$ is about $7 \times 10^{-3}$ in the subcentimeter region.

## 4. CONCLUSIONS

Taking together, we demonstrate the interferometry technique for the refractive index measurements at subcentimeter wavelengths. In contrast to existing resonant methods, which record the interference pattern by a wavelength sweeping, the registration of the interference fringes in our laboratory setup is performed at the fixed wavelength of the coherent radiation. The method is based on a path-length sweeping being introduced into one of the interferometer arms, whereas the sample is tilted out of its normal position with respect to the incident electromagnetic radiation. The determination of the refractive index is realized through the recording of the interference patterns at several tilt angles. The laboratory setup has been tested for several selected materials, both amorphous and crystalline ones.

## REFERENCES


1. J. Krupka, S. Pietruszko, R.G. Geyer, J. Baker-Jarvis, and K. Derzakowski, Measurement of the complex permittivity of microwave circuit board substrates using split dielectric resonator and reentrant cavity techniques, Proc 7th Int Conf Dielectr Mater Meas Appl (1996), 21–24.
2. M.N. Afsar, X. Li, and H. Chi, An automated 60 GHz open rezonator system for precision dielectric measurements, IEEE Trans Microwave Theory Tech 38 (1990), 1845–1853.
3. M.N. Afsar and K.J. Button, Precise millimeter-wave measurement of complex refractive index, complex dielectric permittivity and losstangent of GaAs, Si, $SiO_2$, $Al_2O_3$, BeO, Macor and Glass, IEEE Trans Microwave Theory Tech 31 (1983), 217–223.
4. M.N. Afsar and K.J. Button, Millimeter wave dielectric measurement of materials, Proc IEEE 73 (1985), 131–153.
5. N.N. Almoayed and M.N. Afsar, High-resolution absorption coefficient and refractive index spectra of carbon monoxide gas at millimeter and submillimeter wavelengths, IEEE Trans Instrum Meas 55 (2006), 1033–1037.
6. Z. Abbas, R.D. Pollard, and R.W. Kelsall, A rectangular dielectric waveguide technique for determination of permittivity of materials at W-band, IEEE Trans Microw Theory Tech 46 (1998), 2011–2015.
7. K. Sarabandi, A technique for dielectric measurement of cylindrical objects in a rectangular waveguide, IEEE Trans Instrum Meas 43 (1994), 793–798.
8. O. Tantot, M. Chatard-Moulin, and P. Guillon, Measurement of complex permittivity and permeability and thickness of multilayered medium by an open-ended waveguide method, IEEE Trans Instrum Meas 46 (1997), 519–522.
9. J.R. Birch, Free space video detection of harmonic content of 100 GHz IMPATT oscillator, Electron Lett 16 (1980), 799–800.
10. R. VanLoon and R. Finsy, Measurement of complex permittivity of liquids at frequencies from 60 to 150 GHz, Rev Sci Instrum 45 (1974), 523–525.
11. J. Goulon, G. Rossy, and J.L. Rivarl, Realisation d'un interferometre de Michelson en ondes millimetriques, Rev Phys Appl 3 (1968), 231–236.
12. A.V. Pronin, M. Dressel, A. Pimenov, A. Loidl, I.V. Roshchin, and L.H. Greene, Direct observation of the superconducting energy gap developing in the conductivity spectra of niobium, Phys Rev B 57 (1998), 14416–14421.
13. A.S. Andrushchak and B.G. Mytsyk. Measurement of the refractive indices of isotropic and anisotropic crystalline materials by an interferometric technique, Meas Tech 5 (1992), 33–34.

14. A.S. Andrushchak, B.V. Tybinka, I.P. Ostrovskij, W. Schranz, and A.V. Kityk, Automated interferometric technique for express analysis of the refractive indices in isotropic and anisotropic optical materials, Opt Lasers Eng 46 (2008), 162–167.
15. A.A. Volkov and A.S. Prokhorov, Millimeter-submillimeter BWO spectroscopy of solids, www.submm.gpi.ru, Institute of General Physics, Russian Academy of Sciences, Moscow.
16. B.P. Gorshunov, A.A. Volkov, A.S. Prokhorov, and I.E. Spektor, Methods of terahertz-subterahertz BWO spectroscopy of conducting materials, Phys Solid State 50 (2008), 2001–2012.
17. B.P. Gorshunov, et al., Terahertz BWO spectroscopy of conductors and superconductors, Quantum Electron 37 (2007), 916–924.
18. A.A. Volkov, Yu.G. Goncharov, G.V. Kozlov, S.P. Lebedev, and A.M. Prokhorov, Dielectric measurements in the submillimeter wavelength region, Infrared Phys 25 (1985), 369–373.
19. N.A. Andrushchak, Ya.V. Bobitskii, T.V. Maksymyuk, O.I. Syrotynsky, A.S. Andrushchak, and I.D. Karbovnyk, A new method for refractive index measurement of isotropic and anisotropic materials in millimeter and submillimeter wave range, Proceedings of the 18th International Conference on Microwave, Radar, and Wireless Communications MIKON-2010, Vilnius, Lithuania, 2010, pp. 273–275.